Anisotropy Under Conditions of Plane Strain," *Journal of the Mechanics and Physics of Solids*, Vol. 20, pp. 239–253.

Guo, Q., and Keer, L. M., 1990, "A Crack at the Interface Between an Elastic-Perfectly Plastic Solid and a Rigid Substrate," *Journal of the Mechanics and Physics of Solids*, Vol. 38, pp. 843–857.

Mohan, R., Ortiz, M., and Shih, C. F., 1992a, "An Analysis of Cracks in Ductile Single Crystals—I. Anti-Plane Shear," *Journal of the Mechanics and Physics of Solids*, Vol. 40, pp. 291–313.

Mohan, R., Ortiz, M., and Shih, C. F., 1992b, "An Analysis of Cracks in Ductile Single Crystals—II. Mode I Loading," *Journal of the Mechanics and Physics of Solids*, Vol. 40, pp. 315–337.

Rice, J. R., 1973, "Plane Strain Slip Theory for Anisotropic Rigid-Plastic Materials," *Journal of the Mechanics and Physics of Solids*, Vol. 21, pp. 63–74.

Rice, J. R., 1987, "Tensile Crack Tip Fields in Elastic-Ideally Plastic Crystals," *Mechanics of Materials*, Vol. 6, pp. 317–335.

Shield, T. W., and Kim, K. S., 1991, "Diffraction Theory of Optical Interference Moire and a Device for Production of Variable Virtual Reference Gratings: A Moire Microscope," *Experimental Mechanics*, Vol. 31, pp. 126–134.

An Analysis for the Effects of Compressive Load Excursions on Fatigue Crack Growth in Metallic Materials

G. A. Kardomateas[10,11] and R. L. Carlson[10,12]

1 Introduction

The variable amplitude loading of service load spectra often includes compressive excursions. Since it seemed reasonable to assume that compressive loads do not induce opening of the crack and hence do not contribute to crack growth, it had been recommended that analyses of crack growth may exclude the compressive excursions, i.e., only cycles with tensile loading need to be included. However, a number of experimental investigations on the effects of compressive excursions indicated that neglecting them can be expected to lead to nonconservative crack growth predictions (Carlson and Kardomateas, 1994).

Based on elastic compression of the asperities, single asperity models had been presented by Beevers et al. (1984). These discrete asperity models provide a rational explanation of the observed behavior due to closure obstruction in load sequences that involve cycling in tension with a positive load ratio, and involve mostly elastic loading/unloading of the asperities. For compressive excursions of sizable magnitude, an inelastic model accounting for the plastic crushing of the asperities is required.

2 Formulation

For a properly loaded specimen, the distribution of the asperities is essentially uniform across the specimen thickness. This suggests the possibility of representing the asperities configuration through the thickness by an effective (through-thickness) line contact.

[10]School of Aerospace Engineering, Georgia Institute of Technology, Atlanta, GA 30332-0150.

[11]Associate Professor, Mem. ASME.

[12]Professor Emeritus.

Contributed by the Applied Mechanics Division of THE AMERICAN SOCIETY OF MECHANICAL ENGINEERS for publication in the ASME JOURNAL OF APPLIED MECHANICS. Manuscript received by the ASME Applied Mechanics Division, Apr. 21, 1993; final revision, Apr. 26, 1994. Associate Technical Editor: R. M. McMeeking.

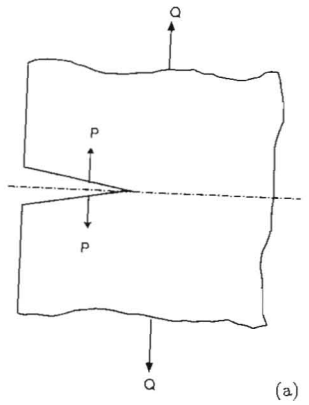

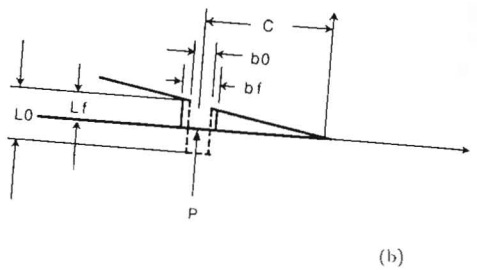

Fig. 1 (*a*) External (global) and crack tip (local) loading; (*b*) a single asperity on the upper crack face

Consider an asperity at a distance C from the crack tip in a specimen of thickness t (Fig. 1). The presence of both externally applied forces and crack face forces is illustrated in Fig. 1(*a*) whereas the details of the proposed model are indicated in Fig. 1(*b*). Only the upper crack face is shown with the asperity developing a force P. The stress intensity factor produced by concentrated, opposing line loads on the faces of a finite center crack of length $2a$, can be determined from Sih et al. (1962) for both the Mode I and Mode II cases. The opening mode stress intensity factor for plane strain in terms of the local crack face force from Sih et al. (1962) is

$$K_{I,\text{local}} = \left(\frac{1}{\pi C}\right)^{1/2}\left(2 - \frac{C}{a}\right)^{1/2}\frac{P}{t}. \tag{1}$$

This expression is also valid for a single-edge crack of length a (this can be easily shown by following the same procedure as in Sih et al., 1962).

The contribution of the external load will be represented by $K_{I,\text{global}}$. By superposition, the total stress intensity factor is

$$K_I = K_{I,\text{local}} + K_{I,\text{global}}. \tag{2}$$

The dimension L_0 represents the initial magnitude of the interference produced by the asperity. The effective initial width of the asperity is b_0 (Fig. 1(*b*)). The load P will now be determined from a displacement condition at the asperity site, which includes the plastic crushing of the asperity.

The vertical displacement at the upper crack face, i.e., at $\theta = \pi$ and an arbitrary r, is

$$U_2(r, \pi) = U_{2,\text{global}} + U_{2,\text{local}}. \tag{3}$$

By use of the stress intensity factors for the global and the local load, we can write the displacement at the asperity site, $r = C$, $\theta = \pi$:

$$U_2(C, \pi) = \frac{2}{G}\left(\frac{C}{2\pi}\right)^{1/2}(1-\nu)K_{I,\text{global}} + \frac{2(1-\nu)}{\pi G}\left(1-\frac{C}{2a}\right)^{1/2}\frac{P}{t}, \quad (4)$$

where G is the shear modulus and ν the Poisson's ratio. The condition for determining the force P is the displacement at the asperity site

$$U_2(C, \pi) = L_f, \quad (5)$$

where L_f is the interference height for a given external load during closure. This will be considered next.

The asperity is assumed under uniaxial compression $\sigma_{22} = \sigma$ (all other stress components are zero). Moreover, the total equivalent strain of the asperity is

$$\bar{\epsilon}^T = \bar{\epsilon}^e + \bar{\epsilon}^p, \quad (6)$$

where $\bar{\epsilon}^e$ is the elastic and $\bar{\epsilon}^p$ the plastic component (we consider positive the asperity stress σ and strain ϵ when they are compressive). Notice that in uniaxial compression, although there are other nonzero components of strain, namely, $\epsilon_{11} = \epsilon_{33} = -\epsilon_{22}/2$, it turns out that $\bar{\epsilon} = \epsilon_{22}$. Hence, since $\bar{\epsilon}^e = \sigma/E$, $\bar{\epsilon}^T = \ln(L_0/L_f)$, the plastic component is

$$\bar{\epsilon}^p = ln\,\frac{L_0}{L_f} - \frac{\sigma}{E}, \quad (7)$$

where E is the modulus of elasticity. Assume now an equivalent true stress vs. integrated equivalent plastic strain law

$$\bar{\sigma} = \sigma_0(\epsilon_0 + \bar{\epsilon}^p)^n. \quad (8)$$

The two constants σ_0, and n are found from two points on the stress-strain curve beyond yield, usually the maximum load and the fracture point, whereas ϵ_0 is found from the yield point, i.e., $\epsilon_0 = (\sigma_Y/\sigma_0)^{1/n}$. The constant n is the strain-hardening exponent. Notice that $\bar{\sigma} = \sigma$.

Next, denote by $A_0 = tb_0$ the initial cross-sectional area of the asperity. For simplicity, we shall consider the material as being incompressible in both the elastic and the plastic ranges when cross-sectional area calculations are performed (this would be strictly accurate if the Poisson's ratio is 0.5; however, the error introduced for the usual value of 0.3 can be reasonably expected to be small, if the elastic strains are small compared to the plastic ones). Therefore, the incompressibility requirement gives a relationship for the current cross-section A_f and the stress $\sigma = P/A_f$:

$$A_f L_f = A_0 L_0, \quad \sigma = \frac{PL_f}{A_0 L_0}. \quad (9)$$

Using (7), (8), and (9) gives one equation in P, L_f:

$$\left[\frac{PL_f}{\sigma_0 A_0 L_0}\right]^{1/n} = \ln\frac{L_0}{L_f} - \frac{PL_f}{EA_0 L_0} + \epsilon_0. \quad (10a)$$

The other equation needed to solve for L_f and P is found from (4) and (5):

$$L_f = \frac{2}{G}\left(\frac{C}{2\pi}\right)^{1/2}(1-\nu)K_{I,\text{global}} + \frac{2(1-\nu)}{\pi G}\left(1-\frac{C}{2a}\right)^{1/2}\frac{P}{t}. \quad (10b)$$

Notice that the final, crushed asperity width can be found from the volume preservation condition (9) and the transverse strain equality $\epsilon_{11} = \epsilon_{33}$:

$$b_f = b_0\sqrt{L_0/L_f}. \quad (11)$$

The description of the asperity behavior for the two separate phases, i.e., the loading and unloading one, will follow next.

Loading Phase. During the application of the external cyclic load, Q, asperity loading may occur from the initial configuration or it may involve reloading after the asperity has been plastically crushed to a reduced height. Hence, during the decreasing external load cycle (loading the asperity) from a general position (Q_i, $P_i = 0$, L_i, A_i) to a position ($Q_f < Q_i$, P, $L_f \le L_i$, $A_f \ge A_i$), the following conditions may develop:

(a) No asperity contact takes place and $K_I = K_{I,\text{global}}$ if, from (10*b*):

$$\frac{2(1-\nu)}{G}\left(\frac{C}{2\pi}\right)^{1/2}K_{I,\text{global}} > L_i. \quad (12)$$

(b) If asperity contact takes place and during asperity loading (decreasing external load), the asperity compresses below yield, then (10*a*) is replaced with the equation found by setting $\bar{\epsilon}^p = 0$ in (7), or

$$\frac{P}{EA_i} = -\ln\frac{L_f}{L_i} \simeq 1 - \frac{L_f}{L_i}. \quad (13)$$

Then the asperity load and final asperity height are found by eliminating L_f from (10*b*) and (13).

(c) If the foregoing conditions are not met and the asperity loading is taking place in the plastic range, then the system of Eqs. (10) is numerically solved.

The current asperity height, L_i, and cross-sectional area, A_i, have been used in (13) instead of the initial values, L_0 and A_0, respectively, since on reloading after a compressive excursion, the asperity is loaded elastically from the current (crushed asperity) dimensions.

Unloading Phase. During the increasing external load cycle (unloading the asperity to zero asperity load), from a position (Q_f, P_u, L_f, A_f) to a position ($Q_i > Q_f$, $P = 0$, $L_i > L_f$, $A_i < A_f$), we recover not the initial asperity height L_0, but the final compressed one, L_f, plus the change in height that is given by the elastic solution that corresponds to the load P_u at which unloading takes place, $\sigma L_i/E$, i.e.,

$$L_i = L_f + \frac{P_u L_f}{EA_f}; \quad A_i = L_0 A_0/L_i. \quad (14)$$

Notice that L_i is now the "new" (after unloading) interference height.

3 Model Predictions

Consider a metal with the mechanical properties: $E = 200$ GN/m^2, $\nu = 0.3$, yield strength $\sigma_y = 400$ MN/m^2, strain-hardening exponent $n = 0.30$ and the constant of Eq. (8), $\sigma_0 = 700$ MN/m^2. The other constant in the relation (8) that describes the behavior beyond yield is found by fitting the yield point, i.e., $\epsilon_0 = (\sigma_y/\sigma_0)^{1/n}$. These material constants are typical of a hot rolled steel. A single-edge-cracked specimen of thickness $t = 13$ mm and width $w = 26$ mm with a crack of length $a = 11$ mm is assumed.

For this case of single-edge through crack of length a in a plate of width w under uniform remote normal load Q, the stress intensity factor is (e.g., Hellan, 1984):

$$K_I(Q) = \frac{Q}{wt}\sqrt{\pi a}\left(1.12 - 0.23\frac{a}{w} + 10.6\frac{a^2}{w^2} - 21.7\frac{a^3}{w^3} + 30.4\frac{a^4}{w^4}\right). \quad (15)$$

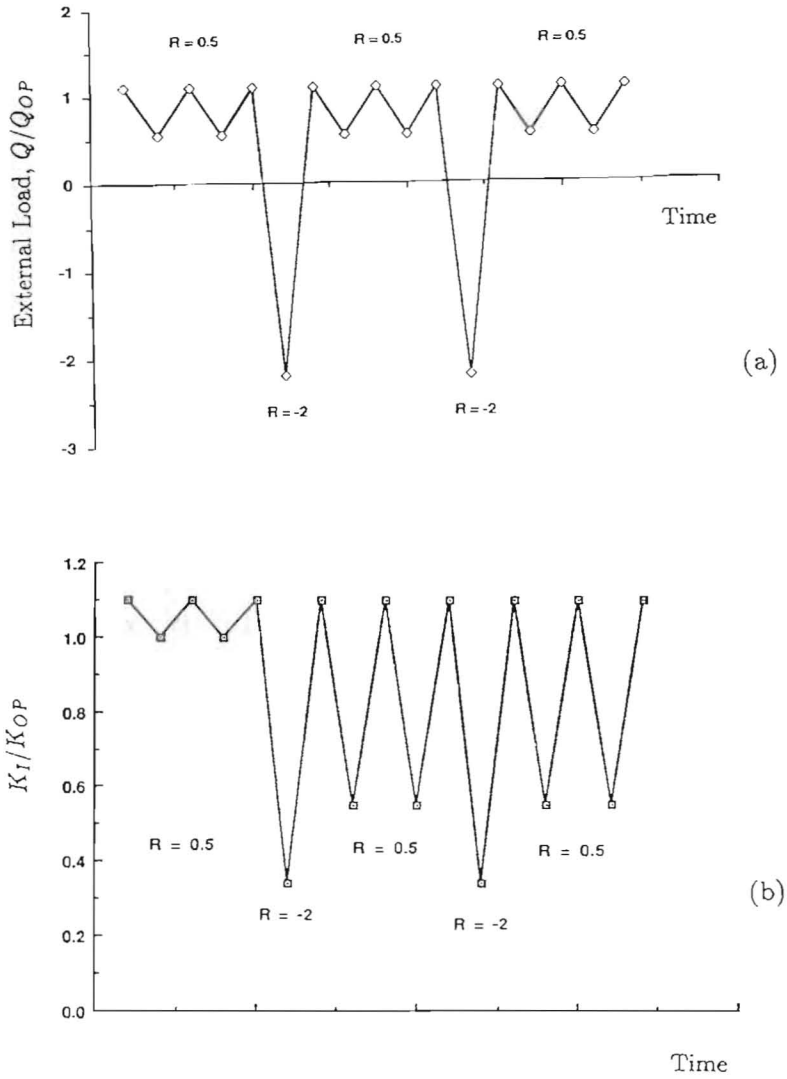

Fig. 2 (*a*) Applied load sequence; (*b*) the total stress intensity factor at different moments during the application of the load sequence

Consider a single asperity configuration with an initial interference height $L_0 = 25$ μm and initial width $b_0 = 50$ μm. The distance from the crack tip is $C = 15$ μm. These are typical dimensions of experimentally observed asperities as reported by Beevers et al. (1984). First, the opening load (load at which asperity contact is established), Q_{OP}, is found by setting $P = 0$ in (10*b*):

$$K_{OP} = \frac{L_0 G}{2(1-\nu)}\left(\frac{C}{2\pi}\right)^{-1/2} = K_I(Q_{OP}). \quad (16)$$

A load sequence as shown in Fig. 2(*a*) is applied. First, the specimen is cycled between $1.1Q_{OP}$ and $0.55Q_{OP}$, so that the load ratio is positive, $R = 0.5$. Then a compressive excursion to $-2.2Q_OP$, i.e., a negative $R = -2$, is applied. Subsequently, the initial, positive $R = 0.5$ is resumed.

The quantity that controls the fatigue crack growth rate is the range in the total stress intensity factor ΔK. Figure 2(*b*) shows the total stress intensity factor at the different stages of the loading sequence. In all segments, at the maximum positive external load, $K = K_{I,\text{global}}$ and the range ΔK is affected by the minimum (positive or negative) external load, at which asperity contact may develop, and a nonzero $K_{\text{I,local}}$ may be generated. At the first $R = 0.5$ load segment, ΔK is relatively small (because of the rather large $K_{I,\text{local}}$ at the load minimum). During the compressive excursion, which crushes the asperity, ΔK is increased substantially. Notice that at the minimum, negative load point, K is positive, nonzero.

4 Conclusions

It has been shown that an inelastic, discrete asperities model can be used to demonstate the effect of compressive excursions during fatigue crack growth. By reducing the height of roughness asperities, the effective range of the stress intensity factor is increased. Subsequent increases in crack growth rate can then be expected to follow.

Acknowledgments

The studies which led to the preparation of this paper were initiated during the support of the Warner Robins Air Logistics Center, Robins AFB under Contact No. F09603-91-G-0096-0013. The authors are grateful for the encouragement provided by the Project Monitor, Mr. Gary Chamberlain.

References

Beevers, C. J., Carlson, R. L., Bell, K., and Starke, E. A., 1984, "A

Model for Fatigue Crack Closure," *Engineering Fracture Mechanics*, Vol. 19, pp. 93–100.

Carlson, R. L., and Kardomateas, G. A., 1994, "Effects of Compressive Load Excursions on Fatigue Crack Growth," *International Journal of Fatigue*, Vol. 16, pp. 141–146.

Hellan, K., 1984, *Introduction to Fracture Mechanics*, McGraw-Hill, New York.

Sih, G. C., Paris, P. C., and Erdogan, F., 1962, "Crack-Tip Stress Intensity Factors for Plane Extension and Plate Bending Problems," ASME JOURNAL OF APPLIED MECHANICS, Vol. 29, pp. 306–312.

An Alternative Derivation of Some New Perspectives on Constrained Motion

A. A. Barhorst[13]

An alternative derivation of some recently reported results is presented. Specifically, some results regarding the fundamental view of Lagrangian mechanics and nonholonomic constraints.

Introduction

In a recent paper (Udwadia and Kalaba, 1992), the general nonholonomic equations of motion for rigid bodies were developed via a constrained optimization procedure. The authors utilized the theory of generalized inverses for matrices. The resulting evolution equations were cast as an error equation similar to state feedback in the modern control theory. The authors mentioned that this interpretation of the nonholonomic dynamics is new and enlightening.

In this Note, the intent is to show that the error type interpretation is also available from a physical formulation of the nonholonomic equations of motion. The presentation herein is more restrictive than the work in (Udwadia and Kalaba, 1992), but it does appear to cover all the cases that arise in engineering systems.

Derivation

Without loss of generality and to facilitate brevity, suppose a system of P particles with N degrees-of-freedom is undergoing holonomic motion, uniquely described by N-independent generalized coordinates. D'Alembert's principle for this system of particles can be written as

$$\sum_p {}^N\delta^o\mathbf{r}^p \cdot \left(\mathbf{F}_p - m_p^o\mathbf{a}_N^p\right) = 0 \tag{1}$$

where ${}^N\delta^o\mathbf{r}^p$ is the absolute variation of the position of the pth particle as seen in the Newtonian frame N with origin o. The vector $\mathbf{F}_p$ is the resultant of forces on the p particle[14], ${}^o\mathbf{a}_N^p$ is its absolute acceleration, and m_p its mass. The vector variation can be written as (Kane and Levinson, 1983; Everett, 1988; Desloge, 1987)

$$\begin{aligned} {}^N\delta^o\mathbf{r}^p &= \frac{\partial^o\mathbf{v}_N^p}{\partial u_n}\delta u_n \\ &= \frac{\partial^o\mathbf{a}_N^p}{\partial \dot{u}_n}\delta u_n \end{aligned} \tag{2}$$

with summation on repeated indices implied. The quantities u_n $(n = 1, 2, \ldots, N)$ are quasi-coordinates or generalized speeds, the simplest choice being the time derivative of the holonomic generalized coordinates $\dot{q}_n$, an alternative choice being a convenient linear combination of the $\dot{q}_n$. With independent variations δu_n, the system's time evolution is modeled with

$$\sum_p \frac{\partial^o\mathbf{v}_N^p}{\partial u_n} \cdot \left(\mathbf{F}_p - m_p^o\mathbf{a}_N^p\right) = 0 \tag{3}$$

for each of the N generalized speeds u_n. Kinematic differential equations relating $\dot{q}_n$ to u_n must also be supplied. If one chooses the simple form $u_n = \dot{q}_n$ for the generalized speeds, then the equations of motion can be written as

$$\boldsymbol{M}(q, t)\ddot{q} = \boldsymbol{Q}(\dot{q}, q, t) \tag{4}$$

where the matrix $\boldsymbol{M}$ has dimension $N \times N$, and $\boldsymbol{Q}$, $\dot{q}$, and q are $N \times 1$ column vectors. The mass matrix $\boldsymbol{M}(q, t)$ and the column vector $\boldsymbol{Q}(\dot{q}, q, t)$ are chosen to be partitioned as follows:

$$\begin{bmatrix} M_{11} & M_{12} \\ M_{21} & M_{22} \end{bmatrix} \begin{Bmatrix} \ddot{q}_m \\ \ddot{q}_{n'} \end{Bmatrix} = \begin{Bmatrix} Q_m \\ Q_{n'} \end{Bmatrix} \tag{5}$$

where

$$\begin{aligned} M_{11} &= m_p \frac{\partial^o\mathbf{v}_N^p}{\partial \dot{q}_m} \cdot \frac{\partial^o\mathbf{v}_N^p}{\partial \dot{q}_m}, \quad M_{12} = \frac{\partial^o\mathbf{v}_N^p}{\partial \dot{q}_m} \cdot \frac{\partial^o\mathbf{v}_N^p}{\partial \dot{q}_{n'}} \\ M_{21} &= m_p \frac{\partial^o\mathbf{v}_N^p}{\partial \dot{q}_{n'}} \cdot \frac{\partial^o\mathbf{v}_N^p}{\partial \dot{q}_m}, \quad M_{22} = m_p \frac{\partial^o\mathbf{v}_N^p}{\partial \dot{q}_{n'}} \cdot \frac{\partial^o\mathbf{v}_N^p}{\partial \dot{q}_{n'}} \end{aligned} \tag{6}$$

and

$$\begin{aligned} Q_m &= \frac{\partial^o\mathbf{v}_N^p}{\partial \dot{q}_m} \cdot \left(\mathbf{F}_p - m_p\mathbf{G}_p\right) \\ Q_{n'} &= \frac{\partial^o\mathbf{v}_N^p}{\partial \dot{q}_{n'}} \cdot \left(\mathbf{F}_p - m_p\mathbf{G}_p\right) \end{aligned} \tag{7}$$

with summation on p implied. The vector $\mathbf{G}_p$ is the gyroscopic terms left after the linear terms in $\ddot{q}$ have been moved to the left-hand side of the equation.

Now consider the same system of particles under the influence of M nonholonomic constraints of the form (Neimark and Fufaev, 1972; Barhorst and Everett, 1993):

$$\delta u_m = A_{mn'}\delta u_{n'}, \quad n' \in \left\{I_i^{N-M}\right\}, \quad m \in \left\{I_d^M\right\} \tag{8}$$

where $\{I_i^{N-M}\}$ means the set of all $N - M$ indices associated to independent generalized speeds. $\{I_d^M\}$ is the set of M indices associated to dependent generalized speeds. Also, $\{I_d^M\} \in \{I_i^{N-M}\}$. The constraint tensor $A_{mn'}$ is a function of the generalized coordinates q and time. Considering Eq. (8), the vector variation in Eq. (1) can be written as

$${}^N\delta^o\mathbf{r}^p = \left(\frac{\partial^o\mathbf{v}_N^p}{\partial u_{n'}} + \frac{\partial^o\mathbf{v}_N^p}{\partial u_m}A_{mn'}\right)\delta u_{n'}, \quad n' \in \left\{I_i^{N-M}\right\}, \quad m \in \left\{I_d^M\right\} \tag{9}$$

with summation on repeated indices. Substitution of Eq. (9) into Eq. (1) allows general conclusions to be drawn.

[13]Assistant Professor, Mechanical Engineering, Texas Tech University, Lubbock, TX 79409-1021. Mem. ASME.

[14]The nonconstraint subset of forces make the ultimate contribution.

Contributed by the Applied Mechanics Division of THE AMERICAN SOCIETY OF MECHANICAL ENGINEERS for publication in the ASME JOURNAL OF APPLIED MECHANICS. Manuscript received by the ASME Applied Mechanics Division, Oct. 12, 1993; final revision, Mar. 21, 1994. Associate Technical Editor: E. J. Haug, Jr.